Regular article

Study of resonant modes in a 700 nm pitch macroporous silicon photonic crystal

D. Cardador, D. Vega, D. Segura, A. Rodríguez

PII: S1350-4495(16)30471-6
DOI: http://dx.doi.org/10.1016/j.infrared.2016.11.004
Reference: INFPHY 2167

To appear in: *Infrared Physics & Technology*

Received Date: 13 September 2016
Revised Date: 10 November 2016
Accepted Date: 12 November 2016

Please cite this article as: D. Cardador, D. Vega, D. Segura, A. Rodríguez, Study of resonant modes in a 700 nm pitch macroporous silicon photonic crystal, *Infrared Physics & Technology* (2016), doi: http://dx.doi.org/10.1016/j.infrared.2016.11.004

STUDY OF RESONANT MODES IN A 700 nm PITCH MACROPOROUS SILICON PHOTONIC CRYSTAL

D. CARDADOR, D. VEGA, D.SEGURA AND A. RODRÍGUEZ

Micro i Nanotecnologies, Departament d'Enginyeria Electrònica, Universitat Politècnica de Catalunya, C/Jordi Girona, 31, 08031, Barcelona, Spain. - E-mail: david.cardador@upc.edu. Tel: +34 93 401 67 66.

ABSTRACT

In this study the modes produced by a defect inserted in a macroporous silicon (MPS) photonic crystal (PC) have been studied theoretical and experimentally. In particular, the transmitted and reflected spectra have been analyzed for variations in the defect's length and width. The performed simulations show that the resonant frequency is more easily adjusted for the fabricated samples by length tuning rather than width. The optimum resonance peak results when centered in the PC bandgap. The changes in the defect geometry result in small variations of the optical response of the PC. The resonance frequency is most sensitive to length variations, while the mode linewidth shows greater change with the defect width variation. Several MPS photonic crystals were fabricated by the electrochemical etching (EE) process with optical response in the range of 5.8 μm to 6.5 μm. Results of the characterization are in good agreement with simulations. Further samples were fabricated consisting of ordered modulated pores with a pitch of 700 nm. This allowed to reduce the vertical periodicity and therefore to have the optical response in the range of 4.4 μm to 4.8 μm. To our knowledge, modes working in this range of wavelengths have not been previously reported in 3-d MPS structures. Experimental results match with simulations, showing a linear relationship between the defect's length and working frequency inside the bandgap. We demonstrate the possibility of tailoring the resonance peak in both ranges of wavelengths, where the principal absorption lines of different gases in the mid infrared are placed. This makes these structures very promising for their application to compact gas sensors.

1. INTRODUCTION

Optical properties of photonic crystals (PCs) are very interesting for a wide range of application areas, such as optical communications or sensing [1]. The particular optical spectrum of a PC is obtained by the periodical ordering of different refractive index materials. The main characteristic of PCs is the occurrence of photonic bandgaps (PBG) at which wavelengths light cannot propagate through the PC. The introduction of defects, that break the periodicity in the structure, confers new optical features to the PC [2]. One example is the embedding of line defects that work as waveguides [3]. Likewise, planar or point defect cavities can be included in a PC. These kind of cavities create resonant states—modes—within the photonic bandgap at specific frequencies [4,5], that are used for the development of optical resonators [6], thermal emitters[7] or tunable filters [8].

As reported in the literature, the crystal's structure, and, in particular, the shape of the defect, influence the optical response of the PC [4]. An important number of papers have dealt with this issue in 1-d and 2-d PCs [9–12]. However, the influence of the defect's morphology on the optical response of 3-d photonic crystals has not been so thoroughly analyzed. This may be due to the high dependence of the optical spectrum on the method used to fabricate the PC [13,14]. A number of different techniques have been proposed to incorporate defect structures within the PCs in woodpile structures [15], synthetic opals [16,17] or macroporous silicon [18], among others.

In this paper we focus on macroporous silicon (MPS), which is a versatile material that can be successfully fabricated by the *electrochemical etching* (EE) of silicon. With this technique it is possible to etch pores with different radius profiles and incorporate planar defects inside the crystal structure, see Fig. 1. Previous studies reported MPS structures with a cavity in the middle of the PC that had a resonant mode around $\lambda = 7\,\mu$m [18]. The reported PC had a pitch of 2 μm and a vertical periodicity of about 2.5 μm. In general, the EE of silicon limits the depth minimum modulation period to be about the lattice pitch for a stable pore growth [19]. The work herein considers PCs with an embedded cavity in the middle. Samples have been fabricated of MPS with a pitch of 700 nm. Vertical periodicities of the samples were close to the lattice parameter, giving a PBG centered at $\lambda \approx 4.5\,\mu$m and with a band-width approximately of 22 %. The included defect was designed for an initial resonance in the range $\lambda = 4.4\,\mu$m to 4.8 μm.

We firstly report the influence that small variations in the defect's length and width have on the resonating modes inside the bandgap. It is shown that there exists an optimal defect shape that ensures the best quality factor as well as that lengthening the defect is a better choice than widening it, to control the frequency of the resonant modes. Experimental data exhibit a linear relationship between the defect's

length and the peak's position inside the bandgap. These results are in good agreement with the results of the theoretical study.

2. EXPERIMENTAL AND SIMULATIONS

Preparation of macroporous silicon PC with defect

Samples of 3-d MPS PC were fabricated using the EE technique, as first described by Lehmann and Föll [20]. An n-type ⟨1 0 0⟩ silicon wafer with suitable resistivity was used to etch pores in a square arrangement with a 700 nm separation. Nano Imprint Lithography (NIL) was used to define the nucleation centers. The 3-d structures were obtained by modulating the currents during EE, thus changing the diameter along the pore depth. This allows to design the profile beforehand and to create smooth, complex 3D structures. An example of the fabricated samples is shown in Fig. 1. The depth periodicity was set to be near 1.1 μm, resulting in a PBG in the range $\lambda = 5\,\mu$m to 7 μm. As seen in Fig. 1, a planar defect was introduced halfway the PC by suppressing one of the modulations and leaving a constant diameter section. The length of the cavity was varied from $l_{\mathrm{def}} = 2.1\,\mu$m to 2.6 μm while the width was set to $w_{\mathrm{def}} = 0.23\,\mu$m for all the samples. To work at shorter wavelengths, the vertical modulation period of the pore was reduced. In particular, it was set to the lattice constant value (~700 nm). This results in a PBG in the range of $\lambda = 4\,\mu$m to 5 μm. The defect's length was adjusted to the range $l_{\mathrm{def}} = 1.5\,\mu$m to 1.8 μm. The total depth of the PC was about 15 μm. A complete description of the process can be found elsewhere [21].

The optical response of the fabricated samples was measured in the MIR range using a Bruker Optic's Vertex 70 FT-IR spectrometer. Measurements were taken with light incidence aligned to the $\Gamma - \mathrm{M}$ direction (along one lattice axis in the surface), an aperture of 1 mm, and a resolution of 4 cm^{-1} was used. Normalized measurements were done for both reflectance and transmittance. Additionally, all measurements are specular.

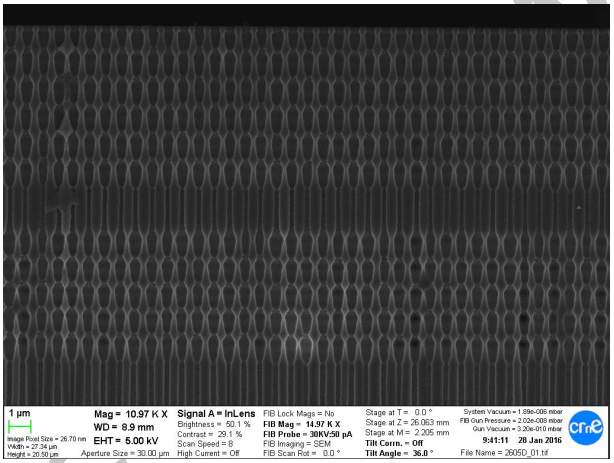

Fig. 1. Cross section view of a 3-d PC fabricated by EE of silicon with a 0.7 μm pitch. A plane defect in the PC lattice is included in the middle of the structure.

Simulations

To study the effects that morphological changes in the defect produce in a finite PC structure, the Optiwave's OptiFDTD software suite was used. This software uses the finite-difference time-domain method (FDTD) to simulate EM wave propagation through a PC, schematized in Fig. 2(a). A single pore was designed using its graphical interface. Each period was inserted in a normalized cell size of 1 µm ×1 µm ×1 µm box –see Fig. 2(a). The pore axis was aligned to the Z axis. Periodic boundary conditions were set on the side walls—*XZ* and *YZ*—while perfect absorbing layers were used for the top and bottom of the simulation cell.

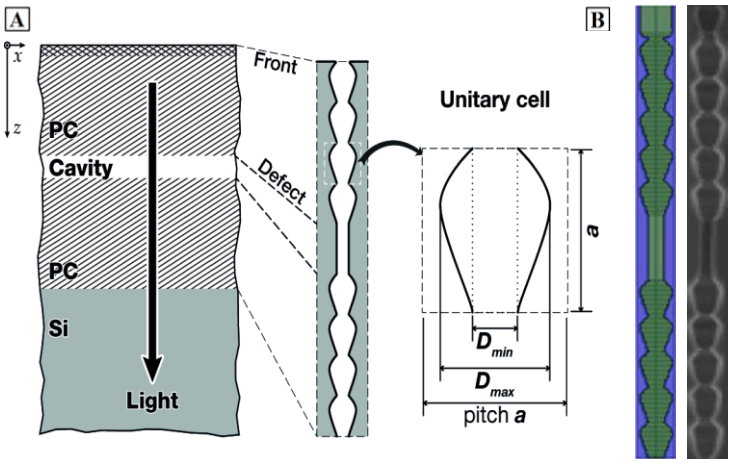

Fig. 2. (A) Schematic representation of the structure and its mode of operation. The unitary cell is one period of the PC in the three space directions. The unitary cell detail gives the principal design parameters. (B) comparison of simulated profile (left), which is a staircase approximation of the experimental profile (right).

The illumination was done with a plane wave arriving from the top and impinging on the front face of the PC. The light wave was a Gaussian pulse with a linewidth of $\Delta = 4\,\mu$m and a central wavelength $\lambda_{\mathrm{src}} = 5.5\,\mu$m. The reflection and transmission spectra were obtained by placing a plane detector $1\,\mu$m and $5\,\mu$m before and after the pore, respectively. Both spectra were calculated by integrating the power flux through the detector plane and normalized to the incident wave.

The refractive index of the bulk material was set to $n \approx 3.43$, which corresponds to the average value of silicon in the mid- infrared range at room temperature [22]. Previous works reported that the absorption in low doped silicon has almost no effect on the propagation of light along the PC [23]. Consequently, in this study no losses were considered in the bulk material. The cavities inside the bulk material were filled with air. The considered PC structure used in the simulations is an approximate geometrical description of the profile depicted in Fig. 1. In concrete, the staircase approximation (see Fig. 2(b)) has been used in order to reduce the morphological differences between both profiles and diminish, as a consequence, the divergence in the optical response between experimental and simulated structures. Several simulations were performed changing the dimensions of the defect site, both length and diameter, to determine the evolution of the cavity mode and the correlation with the measured samples.

3. RESULTS AND DISCUSSIONS

The main results of the theoretical study are summarized in 3; 3 (A) shows the spectra variation of the PC when the length of the defect takes values from 1.6 µm up to 2.4 µm. In 3 (B), the different spectra correspond to a width variation in the range of $0.07\,\mu$m to $0.35\,\mu$m for the mentioned defect. The optimum solution—highest Q-factor—is emphasized with a thicker line, and lies in the middle of the bandgap, in agreement with previous studies made in 1-d and 2-d [24]. Comparing 3 (A) to 3 (B), two differences stand out. The first one is that the central frequency of the resonant mode f_{res} is much more sensitive to changes in the length of the defect than to the width of the defect. A length variation of ± 30 % allows the peak to move anywhere in the PBG. However, in the case of modifying the width, a ± 67 % variation results in a much smaller shift of the peak.

The second difference is higher sensitivity of the resonance Q-factor to changes of the defect's width—widening and thus reducing the Q-factor,—while remaining practically constant with the variation of the length of the cavity. However, the EE fabrication limits for the pore geometry impose restrictions on the realizable PC structures. In particular, too small diameter may lead to pores dying, and too large diameter can result in uncontrolled growth or electropolishing [25]. Considering this, the range of the simulated parameters has been adjusted accordingly. On the other hand, the length of the defect has looser constraints, and can be extended many periods. As observed in Fig. 3(b), it is enough, with the simulated interval, to place the peak at any position inside the bandgap. Nonetheless, further studies should explore the convenience of lengthening the defect. Several reports have demonstrated in 1-d and 2-d that longer defects may allow to excite two or more frequencies that, in turn, will enable the appearance of two or more peaks [26,27].

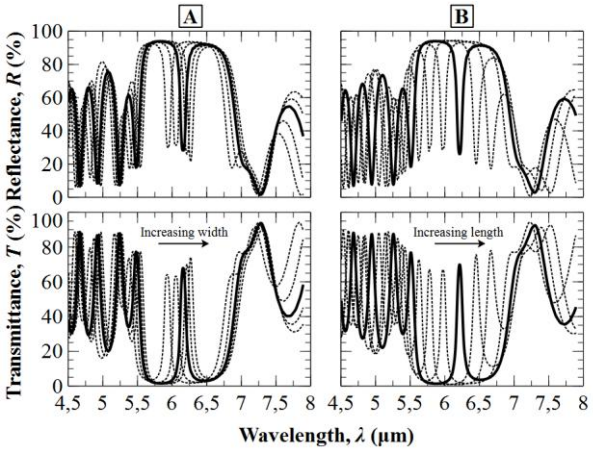

Fig. 3. Reflectance (upper images) and transmitance (lower images) spectra obtained by varying the width (A) and the length (B) of the defect. The length took values from 1.6 μm to 2.4 μm and the with from 0.07 μm to 0.35 μm. In the image it is shown the evolution of the peaks when increaing the size and the length of the cavity. The solid line represents the central —and optimal— frequency, that corresponds to the mean value of the length and the width: 2 μm long and 0.21 μm high.

Taking into account all these considerations, we can conclude that the best way of controlling the position of the peak is to modify the length of the defect, instead of its width. According to this, some MPS PCs were fabricated with different defect lengths to place the resonant mode in the range of $\lambda = 5.8\,\mu$m to $6.5\,\mu$m. In 4(a) is shown the reflectance and transmittance spectra for 3 different samples. It can be observed that the peak's amplitude in the reflectance spectrum matches fairly well with that predicted by simulations. In particular, the simulation data for reflection show that amplitude at the resonance frequency is $R_0^{\text{sim}} \approx 70\%$, while the measured data has $R_0^{\text{meas}} \approx 40\%$. This difference in R_0 and, as a consequence, in the Q-factor, can be attributed to the irregularities in the experimental profile with respect to the simulated one [28–30].

On the other hand, the measured transmitted spectra of the MPS samples are significantly weaker than expected from the simulated results. This is because the PCs fabricated have a total thickness—$250\,\mu$m approximately—of the wafer used as a substrate for the EE: i.e. the PC sits on top of the silicon bulk. Furthermore, the backside of the samples is not polished, so light scattering further reduces the light intensity. A solution that is explored elsewhere [31] is to use MPS membranes, such that the total thickness is substantially reduced.

To achieve shorter wavelengths, several PCs with shorter modulation period were fabricated. As depicted in 4(b), the resonance position could also be tuned, although the features of the cavity modes were a little worse than that obtained in the larger design. The cause is attributed to the increased irregularity of the etched pores. This stems from the added difficulty to control the pore growth when the period approaches the pitch of 700 nm. Even so, these results show the feasibility of working at the range of $\lambda = 4.4\,\mu$m to $4.8\,\mu$m with such MPS PCs.

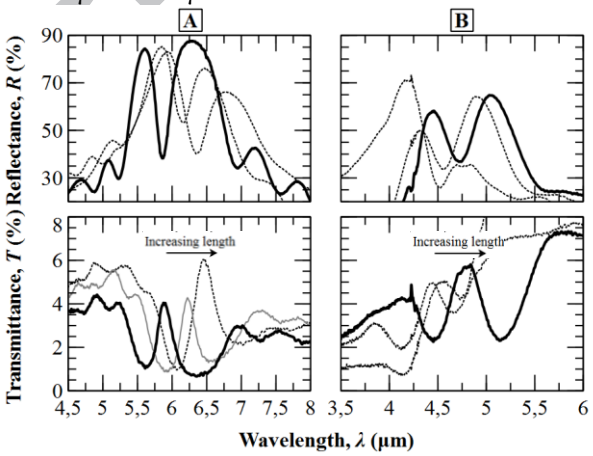

Fig. 4. Experimental spectra of reflection (upper) and transmission (lower) for three different defect length for both cases: (A) 2.06 μm (solid line), 2.34 μm and 2.62 μm (dotted lines). (B) 1.54 μm, 1.60 μm (dotted lines) and 1.76 μm (solid line).

In Fig. 5 the relationship between the defect length and the position of the resonant frequencies is plotted for the long and short period PCs. The center wavelength of the cavity λ_0 is compared for the fabricated and numerically studied PCs. It can be seen that there is some offset for the fabricated samples

with respect to the simulated case. It is suggested that this offset arises because of the difference between the simulation model and the etched pores –see Fig. 2(b). As reported in previous studies, subtle variations in the porosity—volume fraction of silicon over the total unitary cell volume, $p\psi=\neg V_{Si}\triangleleft V_{tot}$—will affect the local effective refractive index, what will generate some modifications in the optical response of the photonic crystal [23]. In concrete, if those differences are given in the defect—i.e. a little eccentricity or roughness in the cavity respect to the perfect cylinder used in simulations—, there will be a shift in the peak position in reference to the ideal case. As seen in Fig. 2(b), the shape of the simulated and experimental pores fit fairly well. However, there are some visible differences between them in both, cavity and modulated zones, such as little variations in the radius and the unitary cell period. These differences may lead to a displacement of the whole bandgap and also a shift in the peak position what, in tum, would produce the offset between the expected and the experimental results. Looking at the slopes in 5, it can be seen that for the larger period samples, there seems to be a good match between theoretical and actual values. However, for the shorter period PCs, the slope for the samples appears to be different from the theoretical one. This may be also attributed to the greater difference of shape in these samples with respect to the desired profile. Further studies are necessary to search how to accurately predict this offset at λ_0. Nevertheless, as λ_0 can be precisely shifted experimentally, this can be used to tune the PC to work at a desired frequency; for instance, at the absorption line of a target gas. Therefore, such MPS devices may be proposed for use as spectroscopic gas sensors.

Tuning the resonances in the mid-infrared range for the long vertical period PCs, allows targeting the absorption spectrum substances such as ammonia, formaldehyde (CH_2O) or the contaminant agent nitrogen dioxide (NO_2). On the other hand, for the short period PCs, it is possible to detect gases involved in industrial processes—such as carbon monoxide, carbon dioxide or nitrous oxide.

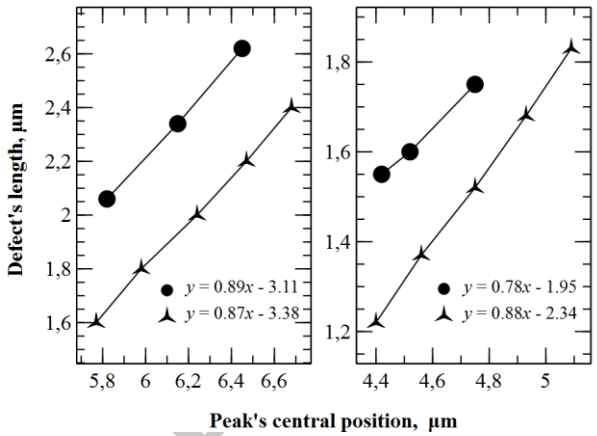

Fig. 5. Experimental (dots) and simulated (stars) relationship between the defect length and the central position of the peak for the two intervals studied: [5.8-6.5] µm (left) and [4.4-4.8] µm (right). They follow a linear regression, written at the bottom of the figure for both cases.

4. CONCLUSIONS

Macroporous silicon photonic crystals with a defect embedded in the middle of the structure have been studied. The PCs have a PBG in the MIR region with a resonance state due to the cavity formed by the defect. The simulations show a shift in the resonating states when we change either the width or the length of the defect and leave the rest of the PC unchanged. Our results show that the defect length is the best option for tuning the resonance position. This helps the design of sharp MIR filters with little variation of the Q-factor for all the tuning range. The relationship between the geometrical variation and the working frequency of the resonating states follows a linear regression.

From the theoretical study, samples with different defect lengths were fabricated with optical response in two wavelength intervals: 7 μm and 4.5 μm. The experimental data show good agreement with the theoretical results in both cases, although some improvements have to be done in further studies to improve the transmission amplitude and the Q-factor of the resonance, especially for the short period samples in the range of 4.5 μm. Finally, we show that MPS PCs are a viable solution for the design of gas detection devices in the mid-infrared, which includes formaldehyde, carbon monoxide, nitrogen dioxide or nitrous oxide, among others.

5. ACKNOWLEDGEMENT

This work has been founded by TEC-2013-48-147-C6-2-R. The authors wish to acknowledge the help from P. Eglitis for his useful comments during the writing of this paper.

6. REFERENCES

[1] C.M. Soukoulis, editor , *Photonic Crystals and Light Localization in the 21st Century* (Springer Netherlands, Dordrecht, 2001).
[2] K. Sakoda, *Optical Properties of Photonic Crystals* (Springer Science & Business Media, 2004).
[3] S.A. Rinne, F. García-Santamaría, and P. V. Braun, Nat. Photonics **2**, 52 (2007).
[4] J.D. Joannopoulos, S.G. Johnson, J.N. Winn, and R.D. Meade, *Photonic Crystals: Molding the Flow of Light (Second Edition)* (2011).
[5] P.V. Braun, S.A. Rinne, and F. García-Santamaría, Adv. Mater. **18**, 2665 (2006).
[6] M. Youcef Mahmoud, G. Bassou, A. Taalbi, and Z.M. Chekroun, Opt. Commun. **285**, 368 (2012).
[7] B. Gesemann, S.L. Schweizer, and R.B. Wehrspohn, Photonics Nanostructures - Fundam. Appl. **8**, 107 (2010).
[8] N. Neumann, M. Ebermann, S. Kurth, and K. Hiller, J. Micro/Nanolithography, MEMS MOEMS **7**, 21004 (2008).
[9] I. Alvarado-Rodriguez, A Diss. Dr. Philos. Electr. … (2003).
[10] X. Xiao, W. Wenjun, L. Shuhong, Z. Wanquan, Z. Dong, D. Qianqian, G. Xuexi, and Z. Bingyuan, Opt. - Int. J. Light Electron Opt. **127**, 135 (2016).
[11] M. Mohebbi, J. Sensors Sens. Syst. (2015).
[12] W. Zhou, D. Zhao, Y.-C. Shuai, H. Yang, S. Chuwongin, A. Chadha, J.-H. Seo, K.X. Wang, V. Liu, Z. Ma, and S. Fan, Prog. Quantum Electron. **38**, 1 (2014).
[13] E. Nelson, (2011).
[14] P.V. Braun, S.A. Rinne, and F. García-Santamaría, Adv. Mater. **18**, 2665 (2006).
[15] M. Taverne, Y. Ho, and J. Rarity, JOSA B (2015).
[16] P. Massé, S. Reculusa, K. Clays, and S. Ravaine, Chem. Phys. Lett. **422**, 251 (2006).
[17] E. Palacios-Lidón, J.F. Galisteo-López, B.H. Juárez, and C. López, Adv. Mater. **16**, 341 (2004).
[18] G. Mertens, R.B. Wehrspohn, H.-S. Kitzerow, S. Matthias, C. Jamois, and U. Gösele, Appl. Phys. Lett. **87**, 241108 (2005).
[19] A. Langner, Doktorarbeit, Martin-Luther-Universität (2008).
[20] V. Lehmann, J. Electrochem. Soc. **137**, 653 (1990).
[21] V. Lehmann, J. Electrochem. Soc. **140**, 2836 (1993).
[22] B.J. Frey, D.B. Leviton, and T.J. Madison, in *SPIE Astron. Telesc. + Instrum.*, edited by E. Atad-Ettedgui, J. Antebi, and D. Lemke (International Society for Optics and Photonics, 2006), p. 62732J–62732J–10.
[23] D. Vega, D. Cardador Maza, T. Trifonov, M. Garin Escriva, and A. Rodriquez Martinez, J. Light. Technol. **PP**, 1 (2015).
[24] M. Mohebbi, J. Sensors Sens. Syst. (2015).
[25] H. Föll, M. Christophersen, J. Carstensen, and G. Hasse, Mater. Sci. Eng. R Reports **39**, 93 (2002).
[26] A. Reynolds and U. Peschel, Microw. Theory … (2001).
[27] S. Lan, S. Nishikawa, Y. Sugimoto, and N. Ikeda, Phys. Rev. B (2002).
[28] M. Minkov, U.P. Dharanipathy, R. Houdré, and V. Savona, Opt. Express **21**, (2013).
[29] Y. Taguchi, Y. Takahashi, and Y. Sato, Opt. Express (2011).
[30] D. Gerace and L. Andreani, Photonics Nanostructures-Fundamentals … (2005).
[31] D. Cardador Maza, D. Vega Bru, D.S. Garcia, T. Trifonov, and Á.R. Martinez, *Enhanced Geometries of Macroporous Silicon Photonic Crystals for Optical Gas Sensing Applications* (2016).

Highlights

- Macroporous silicon photonic crystals with 700 nm of pitch that have a cavity embedded in the middle of the structure have been fabricated and analyzed.
- Samples with different defect lengths were fabricated with optical response in two wavelength intervals: 7 μm and 4.5 μm.
- The relationship between the geometrical variation and the working frequency of the resonating states follows an experimental linear regression, as predicted in simulations, in both studied ranges.
- Although further studies have to be done to improve the figures, this study shows that MPS PCs are a viable solution for the design of gas detection devices in the mid-infrared, which includes formaldehyde, carbon monoxide, nitrogen dioxide or nitrous oxide, among others.